Comparative Study of Time-Resolved Photoluminescence Properties of Terbium-Doped Thiosalicylic-Capped CdS and ZnS Nanocrystals

Carmen Tiseanu,*,† Rajesh K. Mehra,‡ Richard Kho,‡ and Michael Kumke§

National Institute for Laser, Plasma and Radiation Physics, P.O.Box MG-36, RO 76900, Bucharest-Magurele, Romania, Environmental Toxicology Graduate Program, Department of Neuroscience, University of California, Riverside, California 92521, and Institut für Chemie, Physikalische Chemie Universität, Potsdam, Karl-Liebknecht-Str. 24-25, 14476 Golm b. Potsdam, Germany

Received: May 13, 2003; In Final Form: July 23, 2003

We report on the time-resolved photoluminescence (PL) properties of terbium ion doped in CdS and ZnS nanocrystals (NCs). The NCs are capped with thiosalcylic acid (TSA) with size ranging from 3 to 5 nm and studied in aqueous solutions. We found that, although the sensitization of terbium PL in both CdS and ZnS nanocrystals takes place through the same route, namely via the TSA, the dynamics and intensity of terbium PL strongly depend on the nanocrystal type. The observed differences are explained through the different binding modes of the TSA capping molecule with the surface ions of CdS and ZnS nanocrystals. Our results corroborate recent studies on binding of thiol acids with cadmium and zinc chalcogenide nanocrystals.

1. Introduction

In recent years, great interest has been focused on the photoluminescence (PL) properties of nanocrystalline II−VI semiconductors such as CdS and ZnS doped with lanthanide ions ($Ln^{2+/3+}$) such as Tb^{3+}, Sm^{2+}, and Eu^{3+}/Eu^{2+} [1−5] and transition metal ions such as Mn^{2+} [6] because of their interesting optical, magnetic, and photophysical properties.[7−8]

Though most reports claimed that the impurity ions were doped *into* the inorganic core of the NCs, various factors such as mismatch in the ionic radius, charge imbalance, different coordination, as well as differences in chemical properties between the Cd^{2+}, Zn^{2+}, and Ln^{3+} metal ions join to impede the successful incorporation of the lanthanide ions into the inorganic core of semiconductor nanocrystals (NCs).[9] As a result, the actual location of an emissive dopant may vary according to other possibilities as well: trapped in the matrix containing the sample, bound to the surface capping agents, adsorbed onto the surface of the particles, etc.[10]

In contrast with core incorporation, the distribution of the emissive ions on the nanocrystals surface compromise the desired photophysical properties of doped NCs, because of the poor coupling of the emissive ions with semiconductor band electrons, symmetry distortions, and solvent interactions.[10] On the other hand, despite these major drawbacks, the lanthanide ions adsorbed on the NCs surface or bound to the capping ligands can provide useful information on the various interactions taking place in these systems: they can probe for the dynamics of the interfacial electron transfer[11] or for the differences between the binding properties of the capping ligand in free state in solution and those of the capping ligand bound to the nanocrystals surface.[12]

Here we try to demonstrate that the terbium ion bound to a surface ligand such as thiosalicylic acid (TSA) capping two different nanocrystals, namely CdS and ZnS, can probe for the differences between the coordination modes of the ligand with the nanocrystals surface. In the synthesis of both the CdS and ZnS NCs, we took advantage of the bifunctional structure of the TSA acid, to control the surface of the nanocrystals through the thiol group (−SH) and introduce the −COOH functional group with roles in both water solubilization and terbium binding.[13] The investigations were carried out mainly by means of time-resolved photoluminescence spectroscopy on aqueous solutions of terbium-doped CdS and ZnS NCs. It is well-known that the photoluminescence intensity and related lifetimes of the lanthanide ions complexed with organic ligands in aqueous solutions are directly dependent on the number of water molecules bound to their inner coordination sphere; that is, the more efficiently a ligand coordinates to a lanthanide ion, the more water molecules are expelled and consequently, the greater the PL intensity and especially lifetime.[14,15] These effects were used to compare the PL properties of terbium in thiosalicylic capped CdS and ZnS nanocrystals, respectively.

The paper is organized as follows. First, a brief exposition of the TSA molecular structure and its coordination modes toward metal ions is considered. The properties of the absorption and steady-state PL properties of the terbium-doped CdS and ZnS NCs are discussed in connection with their relevant features to the excitation mechanisms and the decays analysis of the terbium PL. Further, preliminary PL decay measurements on the terbium−TSA complex and CdS NCs in the red spectral region are presented. The possible excitation mechanisms of terbium PL in the two NCs are evaluated considering all of the components of the investigated systems: the terbium ion, the organic TSA ligand, and the inorganic CdS and ZnS NCs. As the focus of this study, the terbium PL decays measured in the CdS and ZnS NCs were carefully investigated at several terbium concentrations and emission wavelengths. The interpretation of the distinct dynamics of terbium PL is based on the different luminescent terbium species formed in the two NCs. These species are characterized in terms of the TSA molecular structure and its binding modes toward Cd^{2+} and Zn^{2+} ions on the surface of CdS and ZnS NCs, respectively.

* To whom correspondence should be addressed. E-mail: Tiseanu@totalnet.ro. Phone: + 40 (1) 780 42 90. Fax: + 40 (1) 423 17 91.
† National Institute for Laser, Plasma and Radiation Physics.
‡ University of California, Riverside.
§ Physikalische Chemie Universität.

10.1021/jp035322e CCC: $25.00
Published on Web 10/11/2003

2. Experimental Section

2.1. Synthesis. *Terbium−TSA.* Working solutions of terbium−TSA solutions were solved in deionized water (Millipore). The concentrations of the stock solutions were 10^{-3} and 10^{-4} M for terbium and the TSA, respectively. The terbium concentration was varied between 3.2×10^{-6} and 2×10^{-5} M, whereas the TSA concentration was varied between 10^{-5} and 10^{-4} M, yielding values of 0.03 to 2 for the terbium/TSA concentrations ratio. A 0.1 M $TbCl_3$ solution was also prepared to measure the lifetime of free, aqueous terbium.

Terbium-doped CdS and ZnS NCs. Series of aqueous colloids of CdS and ZnS solutions were prepared using previously published methods[16] with the thiosalicylic acid used as the stabilizing agent. Starting with a 0.075 M solution of TSA in 1 M Tris, $CdSO_4$ or $ZnSO_4$ solutions were titrated to reach a 2:1 molar ratio of TSA:Cd^{2+} or TSA:Zn^{2+} in a final volume of 2 mL. To these TSA:metal complexes, an appropriate volume of sulfide as 1 M Na_2S was added with vortexing to achieve a S^{2-}/metal ratio of 1.0. After thorough mixing, the samples were sealed and incubated for 60 min at room temperature. Based on absorption spectra, the size of the CdS and ZnS nanocrystals ranged from 3 to 5 nm. Terbium ions were added to the solutions of TSA-stabilized CdS and ZnS NCs with the following values for the TSA/terbium concentrations ratios and samples notation: 0, no terbium; 1, 240/1; 2, 120/1; 3, 60/1. The aqueous solutions of CdS and ZnS NCs were stable for more than 4 months under air storage in the dark and at room temperature. However, the solutions utilized in time-resolved experiments tend to coagulate after several weeks.

2.2. Characterization. *Absorption and Steady-State Excitation and Photoluminescence.* UV/vis absorption spectra were recorded on a Perkin-Elmer double-beam spectrophotometer (Lambda 3) controlled by PECSS software. Steady-state excitation and PL spectra were recorded on a Perkin-Elmer LS50B spectrofluorimeter run by FLDM software.

Time-Resolved Photoluminescence and Data Analysis. For the time-resolved PL measurements on aqueous terbium and terbium-TSA compounds a N_2 laser ($\lambda_{ex} = 337$ nm, 20 Hz, Laser Science Inc.) was used.[12] Time-resolved PL experiments with terbium doped CdS and ZnS nanocrystals were carried out using the 3rd harmonic of a Nd:YAG laser as excitation wavelength (355 nm). The laser pulse width was about 10 ns and the mean energy per pulse was around 5 mJ at a repetition rate of 20 Hz. The output beam was focused onto the 1×1 cm quartz cuvette containing the samples using a quartz lens. The size of the spot laser at the cuvette surface was around 2 mm. The luminescence emission was collected at 90° and focused onto the entrance slit of a monochromator with glass lenses. All experiments were performed at room temperature. The data acquisition was performed via a photon counting analyzer, with a temporal resolution of 10 ns per channel. Typically, 10^3-10^5 counts in a peak channel (CPC) of the decay curve were collected. The experiments were performed in the photon-counting regime to minimize pile-up problems in the decays analysis or avoid saturation regime of the photomultiplier. A limited pile-up rate could not be avoided when measuring terbium PL decays in the CdS NCs. The PL transients were analyzed using a multiexponential function $f(t)$

$$f(t) = \sum_{i=1}^{n} A_i \exp(-t/\tau_i) + B \qquad (1)$$

where A_i is the decay amplitude, B is a constant (the baseline offset), and τ_i is the time constant of the decay. The homemade software is based on a Levenberg−Marquard algorithm.[17,18]

SCHEME 1: Functional Structure of the TSA Molecule

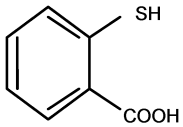

3. Results and Discussion

3.1. Thiosalicylic Acid Binding Modes Toward Cd^{2+}, Zn^{2+}, and Tb^{3+}. TSA is an important ligand in the series of thiol acids with an interesting coordination chemistry that provides both hard and soft donor centers.[13] It can bind to hard metal ions through the carboxylate group and to soft metal ions through the sulfide function (Scheme 1). Although there are some data related to complexes of TSA with divalent alkaline earth metal ions or with transition-metal ions,[13,19] the information is still insufficient to establish the actual modes of binding of the ligands to the metal ions. Most likely, it is the presence of both hard and soft coordinating centers that make difficult the assignment of the actual structure of these molecules.

To our knowledge, the use of thiosalicylic acid as ligand toward lanthanide's ions has not been investigated at all. Such complexes may be interesting in biochemical research as the lanthanide's group, carboxylate functionality, and the sulfide group are biologically important entities.

The lanthanide's ions are known to be highly oxophilic typical "hard" Lewis acids with little affinity for sulfur ligands.[20] Hence, in water, typically only oxygen-containing neutral ligands such as the −COOH group of the TSA acid is considered to bind the terbium ion, because sulfur ligands are not expected to displace the strongly bound water molecules. Recent data[19] on the binding modes of TSA toward the Ca^{2+} ion evidences only binding through the −COOH group of the TSA. We can assume the same for the terbium ion based on the well-known chemical similarities of terbium with Ca^{2+}: besides similar size, bonding, and coordination geometry, both ions show the same order preference for certain donor atoms, oxygen > nitrogen > sulfur.[21] It is therefore reasonable to conclude that in our terbium-doped CdS and ZnS NCs the lanthanide's ion is bound only to the carboxylic group of the TSA capping molecule.

The mechanism of capping CdS or ZnS NCs nanocrystals with TSA organic molecules may be regarded similar to metal ion complexation; that is, a donor−acceptor type interaction between the NCs surface and the ligand site of the organic molecule. Accordingly, the Cd^{2+} and Zn^{2+} ions are expected to bind to both the sulfur and carboxyl moieties of the TSA molecule. However, the affinity of the carboxyl unit toward Cd^{2+} was reported as higher in comparison with Zn^{2+}.[22] Further, it was found that the TSA binds on the CdS NCs surface both as monodentate $(SC_6H_4COOH)^-$ and bidentate $(SC_6H_4COO)^{2-}$ ligand.[23] In the latter mode, TSA binds to the neighboring cadmium ions through both the thiol group and one of the oxygen ions of the carboxylic acid group. The behavior of TSA is further substantiated through contrast with the observed preference of the thio acids that chelate *the same* surface cadmium ion through the oxygen and sulfur bonds.[23]

3.2. Absorption and Steady-State Photoluminescence. *3.2.1. Terbium−TSA.* Figure 1 presents the absorption spectrum of terbium−TSA complex, the excitation spectrum of the aqueous terbium monitored on the terbium 545 nm PL transition, and the PL spectrum of terbium−TSA complex obtained under

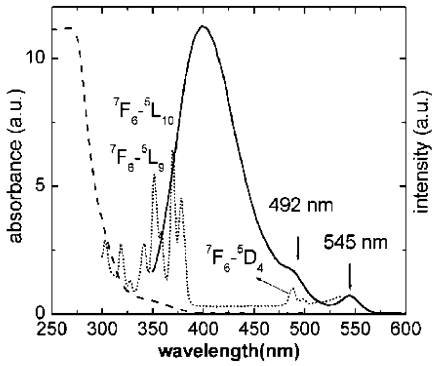

Figure 1. Absorption spectrum of terbium−TSA (dashed line), the excitation spectrum of aqueous terbium PL (dotted line), and the PL spectrum of terbium−TSA complex (solid line). The arrows indicate the terbium PL transitions.

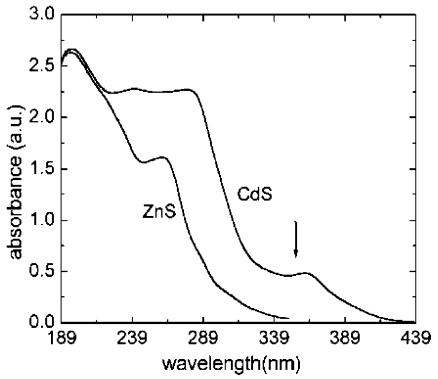

Figure 2. UV−vis absorption spectra of terbium-free CdS and ZnS nanocrystals (samples 0). Arrow indicates the excitation wavelength used in time-resolved experiments (355 nm).

lamp excitation on the maximum of the TSA absorption (290 nm).

The shape of the absorption spectrum of TSA is minimally changed upon terbium complexation, with second-order changes observed in the difference spectrum (not shown). This is not a surprising result as for most carboxylic acids complexation is not detectable in the absorption spectrum.[24]

The PL spectra show the broad, TSA-related PL emission centered on 400 nm with a superimposed structure lying on the red-tail of TSA PL that is readily attributable to the well-known strongest PL transitions of terbium centered on 492 and 545 nm, respectively.

3.2.2. Terbium-Doped CdS and ZnS NCs. Representative absorption and PL spectra of the terbium-doped CdS and ZnS nanocrystals are presented in Figures 2 and 3, respectively. The absorption shoulder at ∼360 nm for the CdS sample is typical for CdS NCs in the 3−5 nm range (Figure 2). In the ZnS sample, absorption is much blue-shifted compared to the CdS NCs, with an absorption maximum near 265 nm. This is also indicative of single-digit nanometer-sized crystals.[16]

The steady-state PL spectra of CdS and ZnS NCs are shown in Figure 3. The emission profile for CdS NCs begins at the absorption tail (∼390 nm), indicating band-edge emissions. The ZnS NCs, in contrast, have PL maxima that are much red-shifted compared to the absorption maxima and can be due to deep trap states in the ZnS core. Upon terbium addition to the CdS NCs, besides the enhancement of the broad, green nanocrystal-related photoluminescence, it is easy to observe a superimposed structure that lies in aprox. 480−650 spectral range. The bands are centered on 492 and 545 nm, which are readily attributed to the 492 and 545 nm centered PL transitions of terbium. In

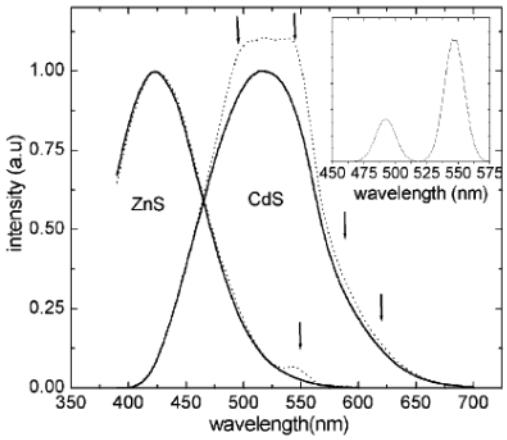

Figure 3. Steady-state PL spectra of terbium-free (samples 0, solid lines) and terbium doped (samples 1, dotted lines) CdS and ZnS NCs. Excitation wavelengths were 380 and 310 nm, respectively (see Figure 2). The arrows point to the emission wavelengths measured in the time-resolved PL experiments. Inset: difference of the PL spectra of ZnS NCs.

ZnS NCs, the lanthanide's characteristic emission appears with a less marked shoulder on the extended red tail of ZnS PL located at ca. 545 nm. The difference spectra better reveals the terbium PL transitions centered on 545 and 492 nm (Figure 3, inset).

We should add here that the terbium addition has complex effects on both the absorption and the steady-state PL of CdS NCs. For instance, although the terbium related PL increases with terbium concentration, the CdS related PL suffers both an enhancement and quenching effect relative to the PL of terbium free CdS. Both effects are selective in nature; that is, only the red part of the CdS PL spectrum is affected upon terbium addition. Details on the terbium induced changes of the optical properties of the CdS NCs make the object of a separate paper that will be submitted elsewhere.

3.3. Time-Resolved Photoluminescence. *3.3.1. Terbium−TSA.* Upon 337 nm excitation, several PL decays of terbium in TSA complexes were measured at the 545 nm based PL transition of terbium. All PL transients were fitted with single exponentials, and the following lifetimes values were obtained: [12] 190 μs, 230 μs, and 260 μs for the concentrations ratio of the TSA/terbium of 2, 1, and 0.5, respectively. When the concentration ratio of TSA/terbium was further decreased to 0.03, the PL was reduced to 160 μs. The lifetime's values of terbium PL in the TSA complex are well below the ca. 385−408 μs values corresponding to lifetimes of free, aqueous terbium measured under identical experimental conditions.

3.3.2. CdS−Red PL. Under 355 nm laser excitation, all CdS samples, regardless of doping and/or terbium concentration, emit both green and red light. The red PL has a broad, featureless spectrum extending from ca. 600 to 800 nm, with the associated intensity considerably weaker than the green PL as revealed by amplitude analysis on the oscilloscope.

Several PL decays were measured within the ca. 600−800 nm range. All decays have a two-decay pattern (Figure 4), with a fast decay value of about 1 μs accounting for more than 70% of the total amplitude and a longer decay value measuring 5−10 μs. Under careful examination of Figure 4, a third, much longer lived decay component with decay values of several tens of μs could be inferred. Its amplitude was found to account for less than 2% from the total decay amplitude. It was also detected a slight variation of the PL transients with the emission wavelength (Figure 4), but the signal-to-noise was too poor to be

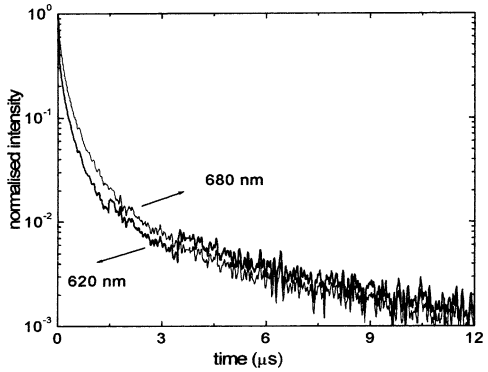

Figure 4. PL decays of CdS nanocrystals measured at 620 and 680 nm. Excitation wavelength is 355 nm.

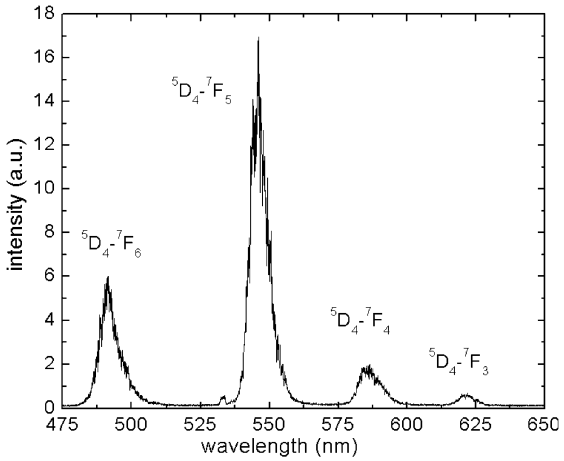

Figure 5. PL spectrum of terbium- doped CdS nanocrystals measured at 100 μs delay after the laser pulse and with a temporal gate width of 3 ms.

further analyzed.[18] As stated recently,[25] a potential application of the existence of the microsecond decay times for the red PL of CdS NCs make these nanocrystals candidates for luminescence probes in the red (or near-infrared) spectral region.

The time-resolved PL data on CdS-related red PL proved useful in the subsequent analysis of terbium PL transients. A similar effect, namely the existence of a long-lived, μs ranged PL, was not evidenced in the ZnS nanocrystals,

3.3.3. Excitation Mechanisms of the Terbium PL in CdS and ZnS NCs. The time-resolved PL of terbium-doped CdS measured at a 100 μs delay after the laser pulse clearly shows the lanthanide's emission spectrum with its characteristic $^5D_4-^7F_J$ ($J = 6, 5, 4, 3$) PL transitions centered on 492, 545, 586, and 622 nm (Figure 5).

Within our instrumental resolution, no quantifiable differences related to the peak values, line shapes, or widths were noticed between the terbium-doped CdS and ZnS NCs. However, at longer delay times after the laser pulse (3 ms), only the PL of terbium in ZnS NCs was still detectable. Also, the PL intensity of terbium in ZnS NCs was found to be up to an order of magnitude more intense than that of the CdS NCs.

Upon UV laser excitation, the following pathways are expected for the excitation of the terbium PL in CdS and ZnS NCS, supported by the absorption spectra of free terbium and the TSA (Figure 1), and the CdS and ZnS NCs, respectively (Figure 2): (i) direct excitation into one of the UV absorption bands of terbium ion, (ii) indirect excitation through the TSA, and (iii) indirect excitation through the nanocrystal.

(i) Direct Excitation into One of the UV Absorption Bands of the Terbium Ion. Although in aqueous solutions the absorbance of the free terbium ion is very weak (<1 M^{-1} cm^{-1}),[26] the 355 nm excitation wavelength of the Nd:YAG laser used in the time-resolved studies could directly excite the intra-4 *f* transitions of terbium from the ground state $^7F_6$ to the $^5L_9$ multiplet (Figure 1). As these transitions are among the strongest within the UV group, a nonnegligible contribution of direct excited terbium ions can be made to the to the total terbium photoluminescence.

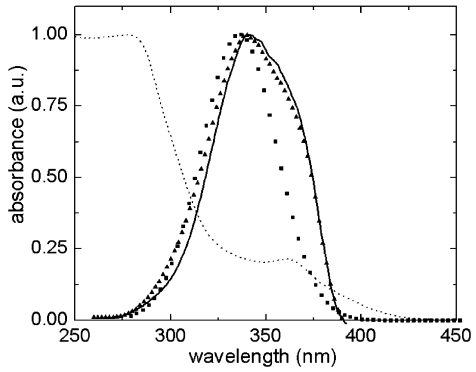

Figure 6. PL excitation spectra of terbium in TSA (▲), free terbium CdS NCs (■) and terbium-PL in CdS NCs (solid line) measured at 545 nm. For comparison only, we included the absorption spectrum of CdS NCs (dotted line) and normalized all of the spectra.

(ii) Indirect Excitation of Terbium PL through the TSA Molecule. Under 355 nm laser excitation, the UV light absorbed by TSA is transmitted to the complexed terbium ion through the intramolecular energy transfer mechanism or IET.[27−29] The ability of the carboxylic acid of the TSA molecule to sensitize the terbium PL was evidenced by the steady-state PL of the lanthanide's ion metal obtained at 290 nm lamp excitation where the absorbance of the free terbium ion could be neglected compared with the TSA absorbance (Figure 1) Two shoulders at 490 and 545 nm attributed to the terbium $^5D_4-^7F_6$ and $^5D_4-^7F_5$ PL transitions can be easily observed as overlapping on the red tail of the TSA photoluminescence. The sensitization of terbium PL through the TSA molecule is further confirmed with the PL excitation spectra of terbium in TSA (Figure 6). The spectrum shape follows the TSA absorption in the range of ca. 275 to 400 nm (Figure 1) with a maximum of intensity at about 340 nm. (Figure 6).

It is generally assumed that IMET in terbium complexes occurs via the triplet state of the organic ligand, though there are few reports on the role of the singlet state of the ligand in mediating IMET[30,31]or on the combination of the both mechanisms.[32]

Probing the donor character of either the singlet or the triplet state by means of time-resolved photoluminescence spectroscopy was not possible because of the limited temporal resolution of the used setup or the lack of observation of the TSA triplet emission or phosphorescence in water solutions and at room temperature.[33] However, for both singlet and triplet mediated IMET, the condition for an efficient energy transfer requires a significant overlap of the TSA fluorescence or PL (singlet emission) or the TSA phosphorescence and the terbium absorption. Although the TSA PL overlaps with the absorption band corresponding to the terbium emissive level, $^7F_6-^5D_4$ (located at 492 nm) through its very low intensity PL tail (Figure 1), TSA phosphorescence that is red-shifted relative to its PL spectra may significantly increase the overlap with the same band.

The efficiency of the IMET from the triplet state of TSA to the terbium ion mainly depends on the ability of TSA in

shielding the terbium ion from the surrounding OH oscillators of the water solvent and the matching between the lowest triplet state of the TSA ligand and the terbium emissive level with the latter condition being as most restrictive. According to the empirical model established by Horrocks,[14] the number of water molecules bound to the inner coordination sphere of the terbium ion has a direct consequence on the decay rate constant of the terbium $^5D_4$ k_{meas}:

$$k_{meas} = k_{rad} + k_{nonrad} + k_{H_2O}\langle sb \rangle \qquad (2)$$

where k_{rad} is the natural radiative rate constant, k_{nonrad} is the rate constant for the radiationless dezexcitation processes which do not involve water and k_{H2O} is the rate constant for the radiationless de-excitation due to the vibrational coupling to the water molecules which is further proportional to the number of water molecules coordinated to the terbium ion. In the absence of the coordinating TSA ligands, the number of water molecules bound to the terbium ion in the inner coordination sphere is about 9,[34] with published values of the luminescence lifetime of the free, aqueous ion varying between 390 and 430 μs.[34,35] Upon terbium complexation with the carboxylic group of the TSA molecules, about one water molecules is expected to leave the inner coordination sphere of the terbium ion which should induce an increase of terbium PL lifetime relative to that measured for free terbium in water. Our results indicate the opposite: the terbium PL lifetimes measured in the TSA range between 190 and 260 μs, well below our measured value of free terbium in water (ca. 408 μs). The results suggest that an efficient quenching process (described with the k_{nonrad} term in eq 2) must be considered, which may be connected with the nonbinding thiol group located adjacently to the carboxylic group in the TSA molecule (Scheme 1).

Other origin of the quenching process may be related to the phonon-assisted back transfer from the terbium emissive level to the triplet state of the TSA. The sensitized PL from terbium is, generally, temperature dependent and results with activation energies consistent with the predicted energy separation between the $^5D_4$ state of the terbium ion and the triplet state of the coordinating ligand. To both realize the energetic requirements and ensure a fast and irreversible (no back-transfer) IMET, a matching condition should be fulfilled i.e., the lowest triplet state energy level of the TSA ligand should be approximately 2000 cm^{-1} higher in energy than the 20 500 cm^{-1} (or 492 nm) $^5D_4$ based terbium emissive level.[36,37] To the best of our knowledge, there are no published data on the triplet energies of the TSA molecule. However, the available data on the terbium complexes with various benzoic acids derivatives show that, for these acids, the matching condition is largely fulfilled. For instance, the triplet energy of the *o*-aminobenzoic that has a $-NH_2$ group situated adjacently to the $-COOH$ group on the phenyl ring is at 25 230 cm^{-1}, with more than 4000 cm^{-1} greater than the energy of the emissive $^5D_4$ level of terbium.[24] To better discriminate the exact nature of the quenching mechanism of the terbium PL lifetime in TSA complex, various terbium−mercaptocarboxylic complexes are currently under investigation.

(iii) Indirect Excitation of Terbium PL through the NCs. As reported, the core incorporation is not necessary for an efficient energy transfer to take place from the nanocrystal to the emissive ions: they may also be excited if they are *closely* located to the nanocrystals surface.[38,39]

We investigated the possibility of the energy transfer from the CdS or ZnS nanocrystals to the terbium ion by means of the excitation spectra. The terbium PL was monitored at 545 nm in both nanocrystals while exciting into the 250−450 nm and 250−400 nm ranges of the CdS and ZnS NCs absorption, respectively (Figure 2).

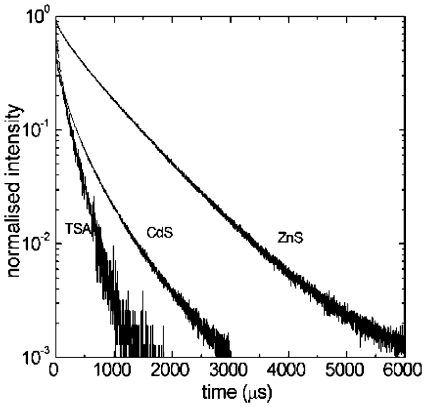

Figure 7. Comparison between the terbium PL decays in TSA, CdS and ZnS nanocrystals. The excitation wavelengths were 337 nm (TSA) and 545 nm (CdS and ZnS NCs).

In ZnS NCs, the PL excitation spectrum of terbium conforms mainly to the shape of excitation spectrum of terbium PL in TSA (Figure 6) with a negligible contribution from the absorption spectrum ofthe nanocrystal. As a result, the possibility of an energy transfer from ZnS NCs to the terbium ion may be ruled out. In CdS NCs, the interpretation of the PL excitation spectrum of terbium is not straightforward because of the strongly overlapping emission spectra of the terbium and CdS nanocrystals at 545 nm (Figure 3) and the similarities in the TSA and CdS absorption spectra (Figures 1 and 2). To illustrate this, we include in the Figure 6, besides the PL excitation spectrum of terbium in TSA, the PL excitation spectrum of terbium free-CdS NCs and the PL excitation spectrum of terbium in CdS NCs. The latter spectrum was obtained as the difference of the PL excitation spectra of the terbium doped CdS NCs (sample 3) and the terbium free-CdS both monitored at 545 nm.

It is readily seen that the PL excitation spectrum of terbium PL in CdS NCs obtained as above is similar with that measured in TSA. Only a very small increase in the intensity of the PL excitation spectrum of terbium in CdS NCs is observed, in the ca. 340−370 nm range. The effect may be attributed to the contribution of both the CdS NCs and TSA absorption in the excitation spectrum as the related spectra show a similar feature in the region of 340 to 370 nm. Errors that arise from the difference procedure should also be considered.We can therefore conclude that similar with ZnS NCs, the sensitization of terbium PL in CdS NCs is made only through the TSA; the effectiveness of the CdS nanocrystal in sensitization of the terbium PL, if any, is negligible.

3.3.4. PL Decays of Terbium in CdS and ZnS NCs. We examine now the terbium PL decays in CdS and ZnS NCs excited at 355 nm. Figure 7 clearly shows that the terbium PL in CdSs NCs is highly nonexpoential and faster compared to that in ZnS NCs. Further, irrespective of the nanocrystal type, the terbium PL is longer lived than that in the TSA complex. Multiple decays were performed with different experimental parameters in order to check for the reproducibility of the results.

In terbium-doped CdS NCs, the decays were measured on all terbium PL transitions centered on 492, 545, 586, and 622 nm (Figure 5). Two up to three exponentials were needed to fit the terbium PL decays. Table 1 summarizes the PL decay parameters recovered by the exponential analysis at different emission wavelengths and terbium concentrations. All decay values are expressed as mean of up to 8 values measured on different days with different samples.

TABLE 1: Dependence of the PL Decay Parameters of Terbium-Doped CdS Nanocrystals on Emission Wavelengths (λ_{em}) and Terbium Concentration (Sample)[a]

λ_{em} (nm)	sam.	decay times (μs) and in paerntheses relative amplitudes (%)		
492	1	40 ±8 (37)	172 ±16 (14)	490 ± 21 (49)
	2	58 ± 6 (24)	198 ± 20 (24)	502 ± 20 (52)
	3	62 ±5 (12)	184 ± 12 (34)	526 ±12 (54)
545	1	52 ± 8 (38)	183 ± 16 (16)	505 ± 19(46)
	2	50 ± 6 (21)	191 ±15 (25)	498 ± 16 (54)
	3	68 ± 6 (14)	198 ± 2 (30)	530 ± 8 (56)
586	3	86 ±11 (44)	406 ± 21(56)	-
622	3	62 ± 14 (62)	382 ± 34 (38)	-

[a] The decay values are given in mean ±standard error of the mean. The amplitudes are given in mean only.

As shown in Table 1, the PL decays measured at 492 and 545 nm are similar and present, with the exception of a short component located around 50 μs, two longer decays centered on 200 and 500 μs, respectively. The amplitude of the middle decay component with values between 172 and 198 μs shows a strong variation at the expense of the fast decay amplitude: it varies from 14% in sample 1 to 34% in sample 3. The component at about 500 μs is highly reproducible with a standard deviation of less than 4% of the mean. Its amplitude varies only slightly with terbium concentration from about 46% in sample 1 to 56% in sample 3.

We now address the origin of the shortest decay component centered on 50 μs. It is the least reproducible component in both decay values (Table 1) and amplitudes (data not shown). As illustrated in Figure 3, the 492 and 545 nm based terbium PL transitions are on the maximum of the CdS-related emission. Although the lifetimes of CdS PL and terbium PL differ from approximately a few ns[40] to hundreds of μs, respectively, which should allow an excellent temporal discrimination, the detection of the delayed terbium PL can be a difficult task. Because the prompt nanocrystal-related PL is with up to several orders of magnitude stronger than the terbium PL, it may cause the ringing the photomultiplier and associated electronics.[41] The effect of ringing to the measured decay is to introduce a false short decay component with distorted amplitude that is centered on ca. 50 μs. This component does not originate from the terbium PL and is not included in our further analysis.

We also measured the terbium PL decays at the 586 and 622 nm. As these transition are superimposed on the red tail of the CdS related PL, we expected a much lower contribution of the CdS-related PL in the terbium PL decay. The fitting results (Table 1) shows that the decays are strongly different from those measured at 492 and 545 nm: they present besides a short decay component with values of up to 80 μs a longer decay component with values ranging between 382 and 406 μs, respectively. The differences relative to the expected values of ca. of 200 and 500 μs obtained at 492 and 545 nm are ascribed to a combination of two factors: the overlap of the long-lived CdS red PL with the 586 and 622 nm based terbium PL transitions (Figure 3) that complicates the terbium decay through adding new decay components (see also Figure 4) and the low quantum efficiencies associated with these transitions (Figure 5). The latter factor limited the signal-to-noise ratio (SNR) of the transients to about $6-10 \times 10^2$. Such low values for the SNR are demonstrated to critically limit the resolution of the exponential analysis when applied to multiple components decays.[18]

Repeating the experiments on different days with the same sample, the emission decay measured at 545 nm changed mostly in its shortest decay component. The reproducibility of both the decay value and amplitude was poor, with standard deviation of more than 25% of the mean on five measurements. In contrast, the longest decay was satisfactorily reproducible with a standard deviation of 8% of the mean. These results may be related to the photochemical instability in solution of the CdS nanocrystals.[42−44] Under ns laser irradiation in UV, the strong size-dependency of the optical properties of the CdS NCs is manifested in variations of the absorbance as well as in changes in the intensity and spectral shift of the emission band. These changes could distort the measured decays at short times through varying the intensity of the prompt CdS-related PL at 545 nm and hence the effect of ringing in measured decay, but they did not influence the terbium PL behavior at longer times.

TABLE 2: Dependence of the PL Decay Parameters of Terbium-Doped ZnS Nanocrystals on Terbium Concentration (Sample) Measured at λ_{em}= 545 nm[a]

sam.	decay times (μs) and in brackets relative amplitudes (%)	
1	392 ± 11 (32)	842 ± 21 (68)
2	402 ± 8 (30)	852 ± 18 (70)
3	411 ± 10 (23)	856 ± 13 (77)

[a] The decay values are given in mean ±standard error of the mean. The amplitudes are given in mean only.

In contrast with CdS NCs, in ZnS NCs, the excitation energy is absorbed mainly by the TSA (Figures 1 and 2) that limits considerably the contribution of the prompt ZnS-related PL in the terbium measured decay. In addition, the 545 nm based PL transition of terbium in ZnS is well discriminated against the emission maximum of the nanocrystal (Figure 3). As the ringing effect was strongly suppressed, a similar short decay component as detected in the terbium PL decays measured in CdS NCs at 492 and 545 nm is not detected in ZnS NCs (Figure 7). There was still found a less than 100 μs component but its amplitude accounts for less than 6% and therefore it was neglected. Two exponentials are finally needed to recover the PL decays with decay times between 392 and 411 μs and 842−856 μs, respectively (Table 2) The decays are highly reproducible, and the listed values should be regarded as representative for all the measured PL transitions (492, 586, and 622 nm).

There is some tendency of increasing the amplitudes of the longest decay time component with terbium concentration similar with CdS NCs (Table 1). As for the weak dispersion of the decay time values with terbium concentration it is mostly attributed to the experimental and errors in the exponential analysis.

Essential to the formulation of any interpretation of the complex terbium PL decays is the initial possibility of terbium binding to sites on the TSA-capped CdS and ZnS nanocrystals. Given that terbium was added in the aqueous solutions of the TSA-capped NCs, after the nanocrystals were formed, three main terbium luminescent species are expected to coexist: (i) Tb^{3+} complexed with free TSA molecules in solution, (ii) Tb^{3+} complexed with TSA bound to the CdS and ZnS NCs surface and (iii) free, aqueous Tb^{3+} ions. As the TSA capping ligand coordinates distinctly with the nanocrystals surface Cd^{2+} and Zn^{2+} ions, the relative contribution of terbium luminescent species to the total PL decay is expected to depend on the nanocrystal type.

The inspection of the PL decay parameters of terbium- doped CdS nanocrystals collected in Table 1 reveals the presence of two decay values varying between 172 and 198 μs and between 490 and 530 μs, respectively. The shorter decay values are in good agreement with the measured terbium PL lifetimes in TSA for a terbium/TSA concentrations ratio smaller than unity. We therefore assign this component to the lifetime of terbium bound

to free TSA molecules in solution. The existence of a large number of free TSA molecules in solution is sustained by the binding modes of the TSA toward the CdS NCs surface.[20] Accordingly, the TSA molecule binds to the surface Cd^{2+} ions as monodentate ligand, via thiol group as well as bidentate ligand, binding to the neighboring surface Cd^{2+} ions through both the thiol and carboxylic groups. As a result of the later binding mode, a significant number of TSA molecules are expected to be present as free ligands in solution available for terbium complexation. The amplitude of this component should be regarded as greatly underestimated because of the effect of CdS-related prompt PL on the terbium PL decay. The longest decay value ranging between 480 and 530 μs is ascribed to terbium bound to TSA capping the CdS nanocrystals. If we consider the thiol group of the TSA as the source for the quenching of the terbium PL lifetime in free TSA, in TSA bound to the nanocrystal, the effect should decrease as the $-$SH is involved in the coordination of the surface Cd^{2+} ions.[12]

In Zns NCs, because of the lower affinity exerted by Zn^{2+} toward the COOH group of the TSA compared to Cd^{2+},[22] the TSA acid bind to the nanocrystals surface mainly through the thiol group.[45] As a result, the majority of the COOH groups of the bound TSA are sticking radially around NCs, providing a high density of surface ligands that can form complexes with the terbium ions. The exponential analysis of the terbium PL decays in ZnS nanocrystals shows two decay components with values ranging between 392$-$411 μs and 842$-$856 μs, respectively (Table 2). The short decay values nicely fit the PL lifetime values found for the free terbium in water. Similar with the CdS NCs case, the long-lived component is ascribed to the lifetime of terbium bound to the TSA-capped ZnS NCs. The lengthening of the terbium decay in ZnS NCs is also associated with an enhancement of the related intensity of about an order of magnitude compared with CdS NCs. As the values for the radiative as well as the nonradiative rate constants of terbium (namely, the k_{nonrad} term in eq 2) are expected to be similar in the two nanocrystals, the observed change of the terbium PL lifetime in TSA bound to CdS or ZnS NCs should result from the different number of the water molecules bound to terbium ion in the inner coordination sphere in the two nanocrystals. Accordingly, the longer decay values measured in ZnS NCs (Tables 1 and 2) suggest that the TSA bound to ZnS NCs is more efficient in shielding the terbium ion from the surrounding water molecules. Further, the inspection of the results collected in Tables 1 and 2 shows that more than 75% of the total number of terbium ions is bound to the TSA-capping the ZnS NCs compared to only 60% in CdS NCs.

The photochemical processes in the terbium doped CdS and ZnS nanocrystals are complex. Manny issues such as the nature of the differences between the coordination properties of the free ligand TSA and those bound to the surface of CdS and ZnS nanocrystals, respectively, the actual flow of the excitation energy between the three components, namely the metallic (the luminescent terbium), the organic (the TSA ligand), and the inorganic (the CdS and ZnS nanocrystals), the reverse effects of the terbium on the spectral properties of the CdS and ZnS nanocrystals need to be investigated. However, our experimental results clearly indicate that the terbium ion bound to the thiosalicylic capping ligand can probe for the different coordination modes of the TSA toward CdS and ZnS nanocrystals.

Also, the investigated compounds were proven to be optically stable, are water-soluble, and show photoluminescence from both the nanocrystal and terbium ion. Other stabilizing molecules capable of providing to terbium ion both a higher PL quantum efficiency and a longer lifetime could be selected. Potential applications of these compounds could make use of the quantum confinement properties of the NCs together with the unique luminescence properties of the lanthanides.

4. Conclusions

Our time-resolved photoluminescence studies on terbium-doped CdS and ZnS nanocrystals capped with thiosalicylic acid reflect strong differences between the terbium PL properties in the CdS and ZnS nanocrystals in terms of both lifetimes and intensity. Compared to the CdS nanocrystals, the terbium PL in ZnS NCs is stronger and presents a slower dynamics. The results are explained on the basis of the different coordination properties of the TSA capping ligand toward the surface Cd^{2+} and Zn^{2+} surface ions.

Acknowledgment. The authors thank Dr. Totea H. for his valuable help in the design of the experimental setup used in the time-resolved photoluminescence measurements of terbium-doped CdS and ZnS nanocrystals.

References and Notes

(1) Morita, M.; Rau, D.; Fujii, H.; Minami, K.; Murakami, S.; Baba, M.; Yoshita, M.; Akiyama, H. *J. Lumin*. **2000**, *87*−*89*, 478.
(2) Kane, R. S.; Cohen, R. E.; Silbey, R. *Chem. Mater*. **1999**, *11*, 90.
(3) Ihara, M.; Igarashi, T.; Kusunoki, T.; Ohno, K. *J. Electrochem. Soc*. **2000**, *147*, 2355.
(4) Kushida, T.; Kurita, A.; Watanabe, M.; Kanematsu, Y. *J. Lumin*. **2000**, *87*−*89*, 466.
(5) Chen, W.; Malm, J. O.; Zwiller, V.; Huang, Y.; Liu, S.; Wallenberg, R.; Bovin, J. O.; Samuelson, L. *Phys. Rev. B* **2000**, *61*, 11021.
(6) Kubo, T.; Isobe, T.; Senna, M. *J. Lumin*. **2002**, *99*, 39.
(7) Bhargava, R. N. *J. Lumin*. **1996**, *70*, 85.
(8) Mikulec, F. V.; Kuno, M.; Bennati, M.; Hall, D.; Griffin, R.; Bawendi, M. G. *J. Am. Chem. Soc*. **2000**, *122*, 2532.
(9) Ageeth, A. B.; Rick van B.; Meijerink, A. *Chem. Mater*. **2002**, *14*, 1121.
(10) Radovanovic, P. V.; Gamelin, D. R. *J. Am. Chem. Soc*. **2001**, *123*, 12207.
(11) Lee, Y. F.; Olshavsky, M.; Chrysochoos, J. *J. Less-Common Met*. **1989**, *148*, 259.
(12) . Tiseanu, C.; Mehra, R.K.; Kho, R.; Kumke, M. *Chem. Phys. Lett*. **2003**, 337 (*1*−*2*), 131.
(13) McCaffrey, J.; Henderson, W.; Nicholson, B. K.; Mackay, J. E.; Dinger, M. B. *J. Chem. Soc., Dalton Trans*. **1997**, 2577.
(14) Horrocks, W. D., Jr.; Sudnick, D. R. *Acc. Chem. Res*. **1981**, *14*, 384.
(15) Beeby, A.; Clarkson, I. M.; Dickins, R. S.; Parker, D.; Royle, L.; de Sousa, A. S.; Williams, J. A. G.; Woods, M., *J. Chem. Soc., Perkin Trans*. **1999**, *2*, 493.
(16) Torres-Martínez, C. L.; Nguyen L.; Kho, R.; Bae, W.; Bozhilov, K.; Klimov, V.; Mehra, R. K. *Nanotechnology* **1999**, *10*, 340.
(17) Press: A. W. H.; Teukolsky, S. A.; Vetterling, W. T.; Flannery, B. P. *Numerical Recipes in C: The Art of Scientific Computing*, 2nd ed.; Cambridge University Press: Cambridge, 1992.
(18) Istratov, A. A.; Vyvenko, O. F. *Rev. Sci. Instrum*. **1999**, *70*, 1233.
(19) Murugavel, R.; Baheti, K.; Anantharaman, G. *Inorg. Chem*. **2001**, *40*, 6870.
(20) Lamture, J. B.; Zhou, Z. H.; Kumar, A. S.; Wensel, T. G. *Inorg. Chem*. **1995**, *34*, 864.
(21) Bünzli, J.-C. G. *Lanthanide Probes in Life, Chemical and Earth Sciences, Theory and Practice*; Bünzli, J.-C. G, Choppin, G. R, Eds.; Elsevier Science Publishers: New York, 1989.
(22) Morel, F. M. M. *Principles of Aquatic Chemistry*; Wiley-Interscience: New York, 1983; p 237.
(23) Løver, T.; Henderson, W.; Bowmaker, G. A.; Seakins, J. M.; Cooney, R. P., *Chem. Mater*. **1997**, *9*, 1878.
(24) Arnaud, N.; Georges, J. *Analyst* **2000**, *8*, 1487.
(25) Lakowicz, J. R.; Gryczynski, I.; Gryczynski, Z.; Murphy, C. J. *J. Phys. Chem. B* **1999**, *103*, 7613.
(26) Sabbatini, N.; Guardigli, M.; Lehn, J. M. *Coord. Chem. Rev*. **1993**, *123*, 201.
(27) Förster, T. *Ann. Phys. (Leipzig)* **1948**, *2*, 55.
(28) Dexter, D. L. *J. Chem. Phys*. **1953**, *21* (5), 836.
(29) Kirk, W. R.; Wessels, W. S.; Prendergast, F. G. *J. Phys. Chem*. **1993**, *97*, 10326.

(30) Crosby, G. A. *Mol. Cryst*. **1966**, *1*, 37.
(31) Alaoui, I. M. *J. Phys. Chem*. **1995**, *31*, 9.
(32) Thorne, J. R. G.; Rey, J. M.; Denning, R. G.; Watkins, S. E.; Etchells, M.; Gree, M.; Christou, M. *J. Phys. Chem. A* **2002**, *106*, 4014.
(33) Tiseanu C., Kumke, M. U.; Frimmel, F. H.; Klenze, R.; Kim, J. I. *J. Photochem. Photobiol. A: Chemistry* **1998**, *117*, 175.
(34) Horrocks, W. D., Jr.; Sudnick, D. R. *J. Am. Chem. Soc*. **1979**, *101*, 334.
(35) Maji, S.; Sundararajan, K.; Viswanathan, K. S., *Spectrochimica Acta Part A* **2003**, *59*, 455.
(36) Sato, S.; Wada, M. *Bull. Chem. Soc. Jpn*. **1970**, *43*, 1955.
(37) Latva, M.; Takalo, H.; Mukkala, V. L.; Matachescu, C.; RodriguezUbis, J. C.; Kankare, J., *J. Lumin*. **1997**, *75* (2), 49.
(38) Sa'Ferreira, R. A.; Carlos, L. D.; Goncalves, R. R.; Ribeiro, S. J. L.; Bermudez, V. d. Z., *Chem. Mater*. **2001**, *13*, 2991.
(39) Selvan, S. T.; Hayakawa, T.; Nogami, M. *J. Non-Cryst. Solids* **2001**, *291*, 137.
(40) Wu, F.; Zhang, J. Z.; Kho, R.; Mehra, R. K. *Chem. Phys. Lett*. **2000**, *330*, 237.
(41) Selvin, P. R.; Xiao, M., *Rev. Sci. Instrum*. **1999**, *70* (10), 3877.
(42) Balogh, L.; Zhang, C.; O'Brien, S.; Turro, N. J.; Brus, L.*Chem. Today* **2002**, *20* (6), 45.
(43) Harruff, B. A.; Bunker, C. E. *Langmuir* **2003**, *19*, 893.
(44) Henglein, A. *Top. Curr. Chem*. **1988**, *143*, 113.
(45) Chan, W. C. W.; Nie, S. M. *Science* **1998**, *281*, 2016.